Preliminary design of a full electric General Aviation aircraft powered with fuel cell: a case study.

Cafiero G.[1], Comunian P.J.[1], Lerro A.[1], Ponti F.[2] & Damiani Ferretti A.N.[2]

[1] Dipartimento di Ingegneria Meccanica ed Aerospaziale, Politecnico di Torino, Torino, ITALY
[2] Dipartimento di Ingegneria Industriale, Alma Mater Studiorum - Università di Bologna, Bologna, ITALY

Abstract

In this work a preliminary analysis of a full electric general aviation aircraft based on fuel cells is performed and the performance of this solution with those obtained with the same aircraft when powered with solid state batteries is compared. For the considered class of aircraft, the results show that the fuel cell-based system can achieve a much greater range with respect to the battery powered system, when constraining the maximum take-off weight (MTOW). In particular, the fuel cell-based solution can achieve values of the range as large as 500 nm, with a mass penalty with respect to the internal combustion engine (ICE) of about 23%, whilst the battery powered solution can only attain values of the range equal to 200 nm with the same MOTW.

Keywords: Full electric aircraft; Fuel cells; Preliminary design; Batteries

1. Introduction

The emission of greenhouse gases is causing a rising global average temperature and extreme climate events. The European Commission has set ambitious goals until 2050 to reduce CO_2 and NO_X emissions in aviation. But to reach these goals revolutionary developments are necessary since the optimization potential of conventional technologies is limited. Propulsion systems powered by proton-exchange membrane fuel cells (PEMFC) emit only water vapor and would reduce the climate impact of aviation. Therefore, the feasibility of hydrogen powered PEMFC propulsion systems for the application in different aircraft categories is analyzed [1]. The recent advancements of companies such as Airbus 0 and ZeroAvia [3] in demonstrating the use of fuel cells for passenger aircraft has given a further burst on the development of the technology.

As a part of the National Centre for Sustainable Mobility (MOST), in this work a study aimed at converting a general aviation aircraft (of the same class of the Cirrus SR-22) in a full electric aircraft powered with fuel cells is performed. The focus is put on the mass penalty of the innovative propulsion system on the general aviation aircraft, comparing the results with a solution fully based on batteries. The study is carried out considering an entry into service of the newly powered aircraft by 2030, hence considering technology with potential improvements that do not exceed 10%.

2. Top level aircraft requirements

For the present investigation, the focus is put on a cross-country mission for a general aviation aircraft of the class of the Cirrus SR-22 [4]. A set of top-level aircraft requirements (TLAR) have been considered, as listed in Table 1. These requirements need to be in line with the reference aircraft [5], with penalties associated with the conversion of the ICE to full electric aircraft. A reduction in the maximum range is allowed (currently considered as 900 nm).

RANGE [NM]	500

MTOW [KG]	1865
RATE OF CLIMB [FT/MIN]	1500
ASPECT RATIO	10
TAKE-OFF DISTANCE [FT]	1300
WING AREA [M^2]	13.4
CRUISE ALTITUDE [FT]	8000

Table 1: List of requirements and assumptions for the general aviation aircraft

For the current investigation, two possible full electric propulsion systems were considered based on fuel cells (FEFC) or on batteries (FEB). It is worth noting that, even in the FEFC case, batteries were considered to accommodate the peak power requirements during the take-off and climb phases. This has been done because fuel cells are characterized by a relatively slow dynamics, which does not allow to comply correctly with sudden load changes, while batteries offer much faster transients, but are negatively affected by their lower specific energy [18,19].

3. Mission analysis

Starting from the TLAR listed in Table 1, an estimate of the power requirements during all the flight phases of the FEFC and FEB aircraft was carried out. Following the recent results evidenced by ZeroAvia, and accounting for a potential technological improvement in the next years, the following fuel cell data were considered:

FUEL CELL TECHNOLOGY	High-temperature Proton-Exchange Membrane Fuel Cell (HT-PEMFC)
CONVERSION EFFICIENCY [%]	55 (average) [12,13,14]
SPECIFIC POWER [KW/KG]	2.5 (stack)
SPECIFIC ENERGY [KWH/KG]	>1.5 (stack)
GASEOUS H_2 TANK PRESSURE [BAR]	700
TANK GRAVIMETRIC EFFICIENCY	7%

Table 2: Fuel cell data

A set of assumptions were made about the performance of the fuel cell system and of the batteries. Starting from the FEFC case, high temperature PEM fuel cells were considered, for several reasons. Firstly, considering an entry into service of the newly powered aircraft by 2030, it has been estimated that the advancements could allow HT-PEMFC technology to reach a sufficient level of development and have a reliable presence on the market. Moreover, this type of fuel cell, as the name suggests, typically operates at temperatures of around 120-180°C, much higher than the ones of conventional LT-PEMFCs (60-80°C) [6]. This is possible thanks to the different materials employed in the membranes, which are able to achieve high proton conductivity without the need for hydration (as a matter of fact, water would evaporate at temperatures above 100°C). The higher operating temperature brings about additional benefits:

- Humidifiers are not needed, being that the membrane's humidification is no longer required for proton conductivity, thus water management is simplified and pumps parasitic losses are reduced;
- The higher latent heat in the outlet streams allows for a downsizing of the radiators, thus lowering the overall volume and weight of the cooling system and of the BoP as a whole;
- Fuels with higher levels of impurities can be used (up to 30000 ppm CO and up to 20 ppm of sulfur without permanent degradation), because at high temperatures the poisoning process on the Pt within the catalyst layer is heavily hindered.

Regarding the efficiency, LT-PEMFCs show efficiencies which vary over time, typically 55% at the Beginning of Life (BoL) and 45% at the End of Life (EoL) [1,9,10]. On the other hand, due to the higher operating temperature, which is related to the device's efficiency, HT-PEMFC are usually characterized by slightly higher efficiencies [12,13,14]. For this reason, an average value of 55% has been considered for this study.

Specific power (SP_{PEMFC}) and energy (SE_{PEMFC}) have been estimated, based on results already achieved for LT-PEMFCs [11] and data provided by ZeroAvia on HT-PEMFCs [3] and considering reasonable advancements in the time frame of the project.

As far as hydrogen storage is concerned, two main options were initially analyzed: gaseous hydrogen pressurized at 700bar or liquid hydrogen. On the one hand, despite the higher gravimetric efficiency of liquid hydrogen tanks (7.5% against 5.8% for current type IV ones for gaseous hydrogen), liquid hydrogen requires to be cooled down to -253.15°C, which is a quite complex process. Moreover, temperature variations may lead to boil-off, which may cause pressure variations and bursts. On the other hand, gaseous hydrogen is characterized by a technology readiness level (TRL) of 9, representing the fact that it is already a mature technology both in terms of infrastructure and storage solutions. In addition, the high pressure allows for fast refueling and once stored, the gaseous hydrogen is ready for use [11,15,16,17]. For these reasons, gaseous hydrogen storage has been selected as the only option for hydrogen storage for this study. Moreover, considering the time frame of the project, it has been considered that future developments will allow to reach a 7% gravimetric efficiency for this kind of solution [15,16,17].

A schematic representation of the propulsion system envisioned is reported in Figure 1.

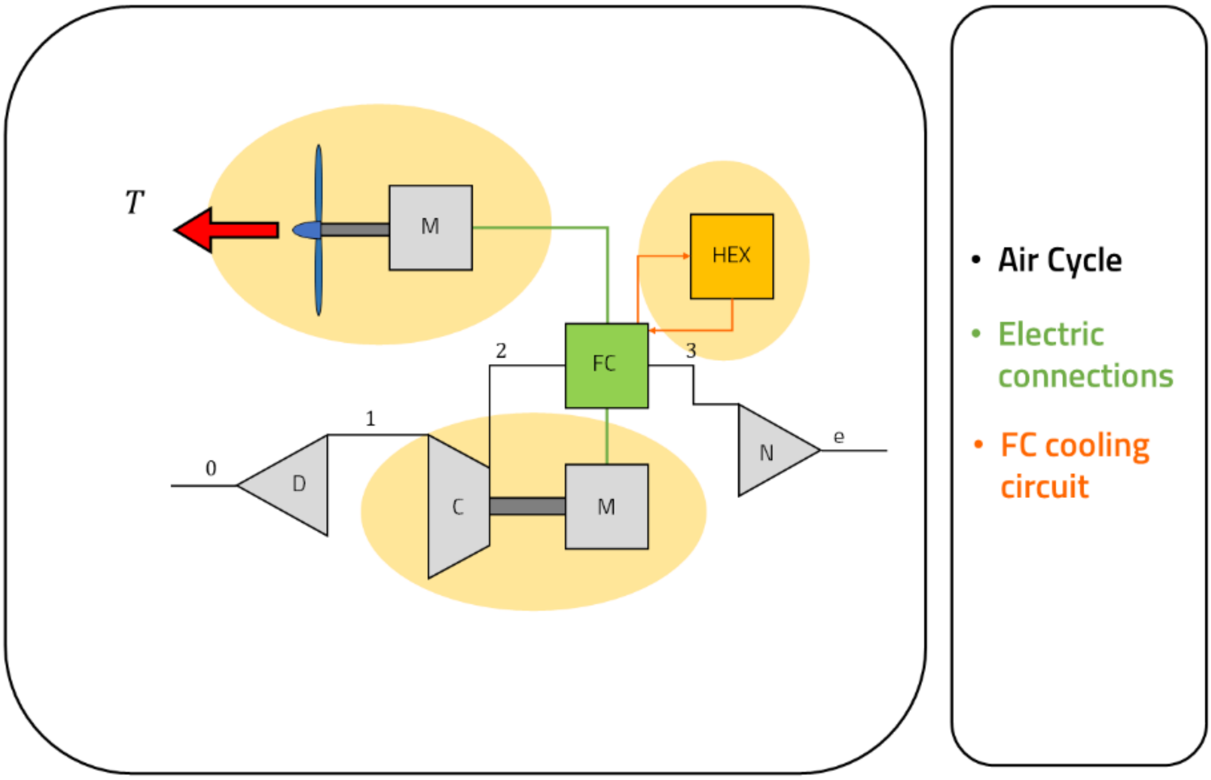

Figure 1: Schematic representation of the fuel cell-based propulsion system

The mission profile of the modified SR-22 aircraft was obtained by implementing an iterative loop (see Figure 2) that started from the data available from the Cirrus SR-22 handbook [5] and then progressively updated the power requirements and the associated MTOW of the aircraft.

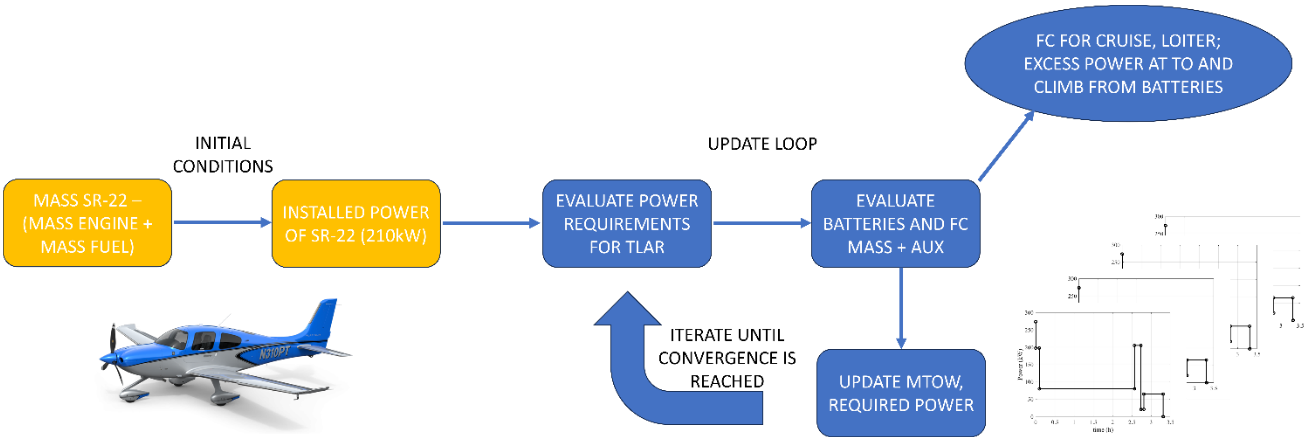

Figure 2: Schematic representation of the iterative loop to update the power requirements and the MTOW of the full electric aircraft based on FC.

The result of the iterative loop in terms of design point is reported in Figure 3 for the fuel cell and battery powered cases. The immediate result is that for a fixed value of the MTOW, the FEFC case can achieve values of the range that are significantly greater than the FEB one.

a) b)

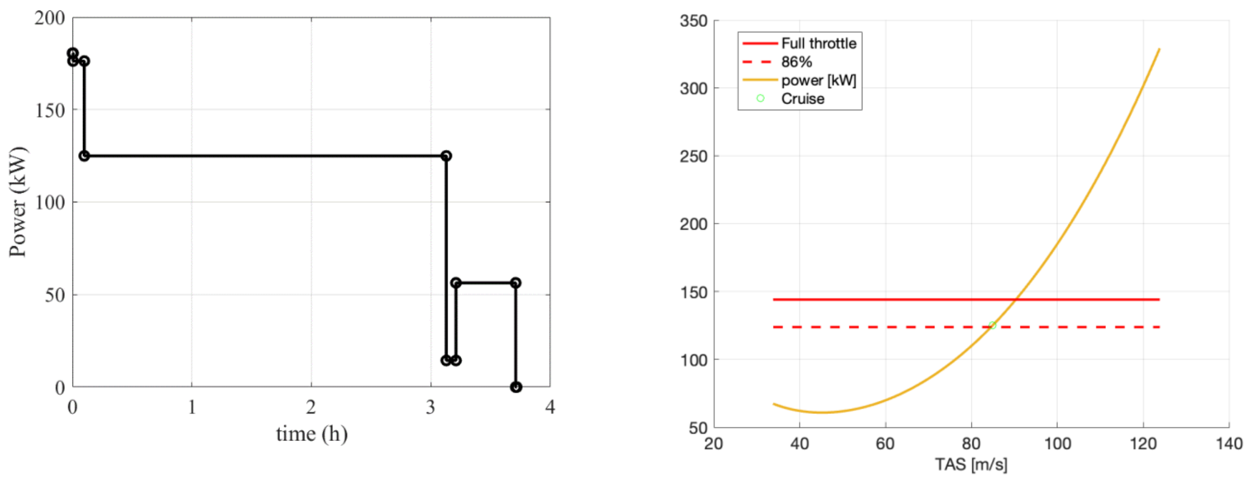

Figure 3: Mission profile (a) and design point (b) for the general aviation aircraft in the FEFC case.

Regarding the sizing process of the fuel cell system, it was based on the power requirement of the cruise phase only, because, as previously stated, fuel cells are characterized by slower dynamics, and batteries were considered to accommodate the peak power requirements during the take-off and climb phases.

For a given required propulsive power ($P_{prop,req}$), a series of losses were accounted for due to the power generation system. Firstly, the propeller was not considered as ideal, thus a propulsive efficiency η_{prop} was introduced to evaluate the required power at the shaft ($P_{shaft,req}$), as shown in Equation (1):

$$P_{shaft,req} = \frac{P_{prop,req}}{\eta_{prop}} \qquad (1)$$

Then, in order to be able to estimate the required fuel cell output power for propulsion ($P_{PEMFC,prop,req}$), as shown in Equation (2), several aspects were taken into account:

- It is assumed that the propulsion power during the cruising phase is not obtained at full throttle. This is represented by $\%_{throttle}$, which is related to the throttle position;
- The electric motor is not ideal. The associated losses are represented by η_{motor};
- The inverter is not ideal. The associated losses are represented by $\eta_{inverter}$;
- There are losses related to the electrical supply line. These are represented by $\eta_{electric}$;
- The product of the last three has been referred to as a stand-alone efficiency (η_i).

$$P_{PEMFC,prop,req} = \frac{P_{shaft,req}}{\%_{throttle} \cdot \eta_{motor} \cdot \eta_{inverter} \cdot \eta_{electric}} = \frac{P_{prop,req}}{\eta_{prop} \cdot \%_{throttle} \cdot \eta_i} \quad (2)$$

Furthermore, a share of the whole available fuel cell output power is used to drive the compressor, required for the fuel cell cathode air supply. This share varies depending on the specific kind of compressor employed [20]. This is represented as a percentage ($\%_{comp}$) related to the required fuel cell output power for propulsion. Finally, the overall available fuel cell output power ($P_{PEMFC,out,req}$) is evaluated as in Equation (3):

$$P_{PEMFC,out,req} = P_{PEMFC,prop,req} + P_{PEMFC,comp,req} = P_{PEMFC,prop,req} \cdot (1 + \%_{comp}) \quad (3)$$

Lastly, to estimate the amount of power that must be stored in the fuel ($P_{inH2inTank,req}$), the conversion efficiency ($\eta_{PEMFC,chem}$) of the fuel cell must be considered. It is related to the conversion of the chemical power stored in the fuel into the output electrical power of the fuel cell.

$$P_{inH2inTank,req} = \frac{P_{PEMFC,out,req}}{\eta_{PEMFC,chem}} \quad (4)$$

Table 3 sums up all the aforementioned contributions in the power estimations.

QUANTITY	[%]
η_{prop}	80 [1]
$\%_{THROTTLE}$	86
η_{motor}	90 [21,22]
$\eta_{inverter}$	98 [23]
$\eta_{electric}$	90
$\%_{COMP}$	10 [20]
$\eta_{PEMFC-CHEM}$ (avg between BoL and EoL)	55 [12,13,14]

Table 3: Efficiencies used during the sizing process

In particular, the result of the update loop leads to an installed power of the fuel cell system $P_{PEMFC,out,req}$ = 250 kW, which yields to a maximum available power from the fuel cell of 125 kW.
In Table 4, a detailed breakdown of power requirements between fuel cell and batteries during each of the FEFC mission profile phases is reported. The batteries allow to accommodate for the gap between the fuel cell power and the required propulsive power during take-off and climb. It is worth to mention explicitly that during the take-off and climb phases the FC is operated at full throttle. While this is not considered as possible for the cruise phase, it is deemed as a reasonable approach for the take-off and climb phases owing to their short time duration with respect to the full flight.

	$P_{PROP,REQ}$ [KW]	$P_{PROP,REQ,FROMPEMFC}$ [KW]	$P_{PEMFC,OUT,REQ}$ [KW]	$P_{BATT,PROP,REQ}$ [KW]
TAKE-OFF	180	144 (at full throttle)	250	56
CLIMB	176	144 (at full throttle)	250	56
CRUISE	125	125	215	0
DESCENT	14	14	28	0
CRUISE	76	76	152	0

Table 4: Power breakdown during the flight phases for the FEFC case.

As it can be seen from the data, the sizing of the fuel cell system is performed on the cruise phase. As reported in Equation (5), the mass of the fuel cell system has been estimated based on power, using the specific energy reported in Table 2:

$$m_{PEMFC} = \frac{P_{PEMFC,out,req,cruise}}{SP_{PEMFC}} \quad (5)$$

On the other hand, Equation (6) reports how the amount of hydrogen required to complete the mission was estimated, as the sum of all the masses of hydrogen required during each phase, and knowing that the hydrogen energy content (SE_{H2}) is equal to 33.33 kWh/kg:

$$m_{H_2} = \sum_{i=1}^{n} \frac{P_{PEMFC,out,req,i} \cdot t_i}{SE_{H_2}}$$

Then, it was possible to estimate the mass of the tank through the tank gravimetric efficiency reported in Table 2. The final value of the total mass of the propulsion system is then increased by an additional 10% to account for the masses of the auxiliary systems. The resulting total mass of the propulsive system associated with the FEFC case is about 792 kg assuming the gravimetric efficiency of the tank equal to 7%.
In the FEB case the power demand is fully accommodated by the use of batteries. leading to a very high (and totally unpractical) total aircraft mass. The calculation is performed keeping the same value of the total aircraft mass as in the FEFC, which inevitably leads to a reduction of the range.
The estimate of the battery mass associated with the FEB case is performed by considering a similar chain of efficiencies as previously reported for the FEFC case, with the except of the efficiency of the auxiliary systems. Indeed, in the FEB case the compressor and heat exchanger will not be employed and as such, those penalties are not being kept in the computation.
Therefore, starting from the power required at the shaft, a first efficiency of the propeller is considered. Secondly, the efficiency of the electric motor is kept in the computation, which leads to the required power of the propulsive system. Assuming an energy density equal to 400 Wh/kg, which is a significative advancement with respect to the batteries available on the market at the moment, the estimated range of the FEB aircraft is equal to 192 nm (approximately 79% less than the ICE configuration). The FEFC case, keeping the same value of the MTOW, is therefore capable to cover a range that is more than doubled compared with the FEB one, although a penalty both in terms of range and of mass ought to be accepted with respect to the ICE case.

	FEFC	FEB
m_{PEMFC} [KG]	100	-
m_{H_2} [KG]	39.7	-
m_{tank} [KG]	565	-
m_{batt} [KG]	15	792
TOTAL MASS [KG]	792	792

Table 5: Mass breakdown of the fuel cell system and required batteries.

4. Allocation of the masses and stability analysis

For the remainder of the manuscript, only the FEFC aircraft shall be considered, owing to the unpractical and inefficient performance of the FEB case. The allocation of the masses is operated starting by the SR-22 ICE aircraft and removing those elements that are not necessary for the FEFC case, such as the mass associated with the fuel and the combustion engine.
The storage of the hydrogen is assumed to be obtained with a combination of one internal spherical tank, and two sub-wing ellipsoidal tanks. The geometric parameters and the corresponding values of the stored hydrogen are reported in table 5, which satisfy the required volume of hydrogen for the mission.

	SPERICAL (INTERNAL)	ELLIPOSIDAL
RADIUS (M)	0.43	0.3
LENGTH (M)	-	1.6
VOLUME (L)	350	340

Table 6: Geometric details of the internal and sub-wing tanks for the FEFC aircraft.

The span location of the sub-wing tanks has been located at y=1.95m according to the following considerations:
- As close as possible to the wing root as to minimize the structural loading;
- Far enough from the root as to allow the normal operations of the main landing gear. Particular emphasis is posed on the necessity to avoid that the sub-wing tanks can touch the ground during the landing phase due to the elasticity of the gear.

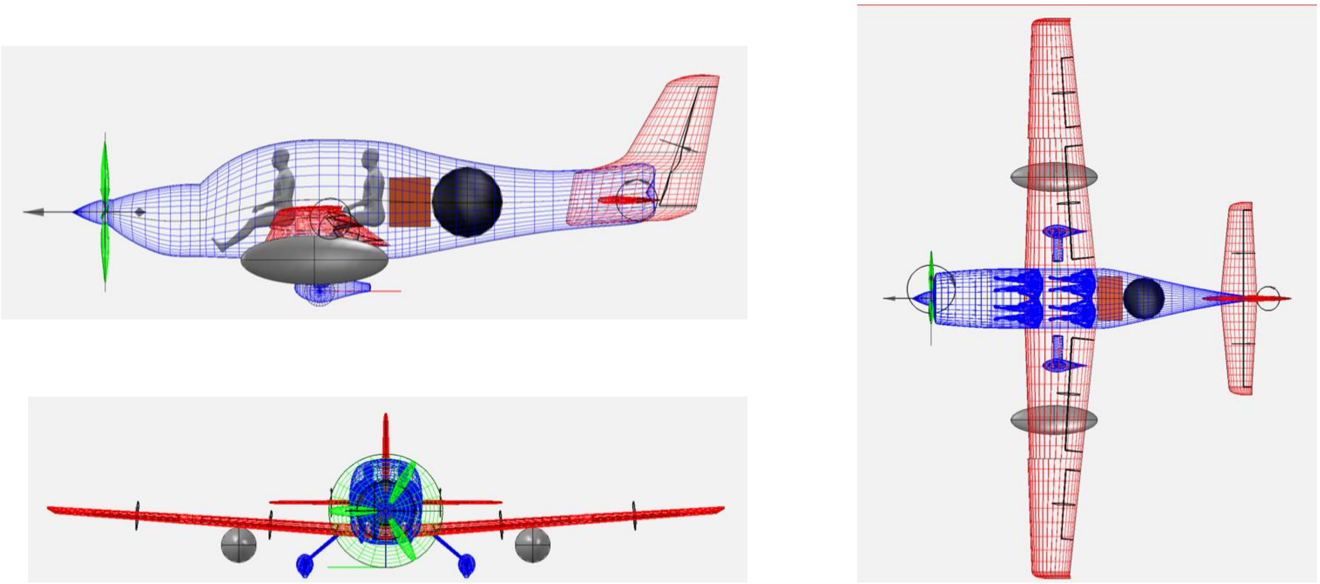

Figure 4: Three-views of the FEFC aircraft with indication of the position of the passengers, internal tank (black sphere), luggage hold (brown paralepidid) and the sub-wing tanks (gray ellipsoids).

The internal tank is located in the rear part of the cabin, towards the tail. While this choice displaces a large mass far from the CG of the aircraft, it allows to include fire-proof walls between the cabin and the tank. Between the internal tank and the cabin there is the luggage hold, which is characterized by a volume of 0.9x0.6x0.5m^3.
Although not explicitly reported in Figure 4, the fuel cells stacks, the electric engine and the inverter are located in the a/c nose replacing the ICE.

Following the approach proposed by Gudmundsson, the location of the neutral point of the vehicle was identified.

$$h_N = h_{ac} + \eta_{HT} V_{HT} \frac{C_{L_{\alpha HT}}}{C_{L_\alpha}} \left(1 - \frac{\partial \varepsilon}{\partial \alpha}\right) \quad (1)$$

with:
h_{ac} = 25% location of the aerodynamic centre (%MAC);
η_{HT} = 1 the efficiency factor of the tail;
$V_{HT} = \frac{S_{HT} l_{HT}}{S_W MAC}$ the volumetric coefficient of the tail;
l_{HT} =3.75m the distance between the aerodynamic centre of the wing and the tail;
$C_{L_{\alpha HT}}$ =4.42 1/rad the slope of the lift curve of the tail
$C_{L_\alpha} = C_{L_{\alpha w}} + C_{L_{\alpha HT}} \frac{S_{HT}}{S_w}$ =6.03 1/rad the slope of the lift curve of the aircraft
$1 - \frac{\partial \varepsilon}{\partial \alpha} = 1 - \frac{2 C_{L_{\alpha W}}}{\pi AR_w}$ downwash factor
The resulting location of the neutral point is h_N =0.55% MAC.
From the SR22-ICE aircraft the location of the CG (h_{CG}) varies between 22.4% and 31.5% of the MAC. The resulting value of the longitudinal stability derivative (C_{M_α}) will vary between -1.4 1/rad and -1.96 1/rad for the rear and aft location of the CG, respectively, where C_{M_α} is obtained as

$$C_{M_\alpha} = C_{L_\alpha}(h_N - h_{CG}) \quad (2)$$

With the removal of the ICE and the introduction of the fuel cells, the two sub-wing tanks and the internal tank, a new location of the CG can be estimated. The total mass of the ICE and the fuel from the SOH is 430 kg.
First, a new location of the centre of gravity of the a/c without the fuel tanks and the ICE has been calculated, accounting for the location and the mass of the removed quantities.
The resulting location of the CG (without the FC system) is h_{CG}=55% MAC. The new location of the centre of gravity is therefore calculated considering the masses (and their location) reported in Table 7.

	$Mass\ (kg)$	$x\ (m)$
ELECTRIC MOTOR + INVERTER	200	1
SUB-WING TANKS	280	2.7
PASSENGERS 2X	160	2.6
PASSENGERS 2X	160	3.7
LUGGAGE HOLD	30	3.88
INTERNAL TANK	188	4.45

Table 7: Mass location in the FEFC aircraft.

The new location of the centre of gravity of the aicraft can be therefore computed as follows:

$$x_{CG} = \frac{\sum_{i=1}^{N} x_i M_i}{\sum_{i=1}^{N} M_i} = 2.99\ m$$

which can be expressed in terms of the MAC as $h_{CG} = 24\%$MAC. Using equation (2) the $C_{M_\alpha} = -1.851$/rad. The proposed mass distribution therefore allows to keep a satisfactory static stability margin.

5. Conclusions and future outlook

The results evidenced by the preliminary design have shown a significant reduction of the achievable range of the FEB case with respect to the FEFC case. This suggests that, for this class of aircraft, the use fuel cells is preferable as it only leads to small reductions of the range, whereas the FEB case would lead to reductions as large as 79% with the same MTOW of the FEFC case.

Nevertheless, the change in the propulsion system poses a series of challenges, including a greater value of the MTOW with respect to the ICE aircraft, by about 23%. Furthermore, the storage of the pressurized hydrogen requires the installation of sub-wing tanks, in addition to an internal spherical tank. This will lead to a detrimental effect on the aerodynamics and structural weight of the aircraft, which requires particular care.

Furthermore, the added mass requires considerations in terms of the flight envelope of the vehicle. If, on the one hand, more aggressive aerodynamics can be envisaged, on the other solutions aimed at the reduction of the friction drag might lead to a benefit on the overall aircraft design.

Acknowledgements

This study was carried out within the MOST – Sustainable Mobility National Research Center and received funding from the European Union Next-GenerationEU (PIANO NAZIONALE DI RIPRESA E RESILIENZA (PNRR) – MISSIONE 4 COMPONENTE 2, INVESTIMENTO 1.4 – D.D. 1033 17/06/2022, CN00000023). This manuscript reflects only the authors' views and opinions, neither the European Union nor the European Commission can be considered responsible for them.

Copyright Statement

References

[1] Schmelcher M, Haby J (2022) Hydrogen fuel cells for aviation? A potential analysis comparing different thrust categories. ISABE-2022-291.

[2] ZeroE: Towards the world's first hydrogen-powered commercial aircraft. url: https://www.airbus.com/en/innovation/low-carbon-aviation/hydrogen/zeroe.

[3] https://zeroavia.com/products-services/

[4] https://cirrusaircraft.com/aircraft/sr-series/

[5] Pilot's operating handbook and FAA approved airplane flight manual for the Cirrus SR-22 (2023)

[6] Ramakrishnan S, Ramya K, Rajalakshmi N (2022) Chapter 10 – High-Temperature Proton Exchange Membrane – An Insight in Kaur G *PEM Fuel Cells – Fundamentals, Advanced Technologies and Practical*

Application (p.p. 223-242). Elsevier. https://doi.org/10.1016/B978-0-12-823708-3.00003-1.

[7] Barbir F (2005) CHAPTER 3 – Fuel Cell Electrochemistry in Barbir F *PEM Fuel Cells: Theory and Practice* (p.p. 33-72). Academic Press. https://doi.org/10.1016/B978-012078142-3/50004-5.

[8] Larminie J, Dicks A.P (2003) Chapter 2: Efficiency and Open Circuit Voltage in Larminie J, Dicks A.P *Fuel Cell Systems Explained*, John Wiley & Sons Ltd. DOI:10.1002/9781118878330.

[9] https://www.plugpower.com/fuel-cell-efficiency-101-the-key-metrics/#:~:text=PEM%20fuel%20cells%2C%20Plug's%20technology,for%20extracting%20power%20from%20fuels.%E2%80%9D

[10] https://www.energy.gov/eere/fuelcells/articles/fuel-cells-fact-sheet

[11] Massaro M.C, Biga R, Kolisnichenko A, Marocco P, Monteverde A.H.A, Santarelli M (2023) Potential and technical challenges of on-board hydrogen storage technologies coupled with fuel cell systems for aircraft electrification. *Journal of Power Sources*, 555. https://doi.org/10.1016/j.jpowsour.2022.232397

[12] Mutlucan Bayat, Mehmet Özalp, Hüseyin Gürbüz (2022) Comprehensive performance analysis of a high-temperature PEM fuel cell under different operating and design conditions. *Sustainable Energy Technologies and Assessments*, 52, Part C. https://doi.org/10.1016/j.seta.2022.102232.

[13] Raj Kamal Abdul Rasheed, Quan Liao, Zhang Caizhi, Siew Hwa Chan (2017) A review on modelling of high temperature proton exchange membrane fuel cells (HT-PEMFCs). *International Journal of Hydrogen Energy*, 42(5). https://doi.org/10.1016/j.ijhydene.2016.10.078.

[14] Li Y, Ma Z, Zheng M, Li D, Lu Z, Xu B. (2021) Performance Analysis and Optimization of a High-Temperature PEMFC Vehicle Based on Particle Swarm Optimization Algorithm. *Membranes*. 11(9). https://doi.org/10.3390/membranes11090691

[15] Huete J, Pilidis P (2021) Parametric study on tank integration for hydrogen civil aviation propulsion. *International Journal of Hydrogen Energy,* (p.p. 37049-37062), 46(74). https://doi.org/10.1016/j.ijhydene.2021.08.194.

[16] Gómez JA, Santos DMF (2023) The Status of On-Board Hydrogen Storage in Fuel Cell Electric Vehicles. *Designs*, 7(4). https://doi.org/10.3390/designs7040097.

[17] Huete J, Nalianda, D, Pilidis, P (2022) Impact of tank gravimetric efficiency on propulsion system integration for a first-generation hydrogen civil airliner. *The Aeronautical Journal*, (p.p. 1324–1332) 126. doi:10.1017/aer.2022.60

[18] Jia, Yaoqin & Wang, Hewu & Ouyang, Minggao (2006) Electric power system for Chinese fuel cell city bus. *Fuel Cells Bulletin*. 155. 12-15. 10.1016/S1464-2859(06)71025-2.

[19] Trilaksono, Bambang & Syaichu-Rohman, Arief & Dronkers, Cees & Ortega, Romeo & Sasongko, Arif (2014) Energy Management of Fuel Cell/Battery/Supercapacitor Hybrid Power Sources Using Model Predictive Control. *IEEE Transactions on Industrial Informatics*. 10. 10.1109/TII.2014.2333873.

[20] Yu, Wan & Sichuan, Xu & Ni, HuaiShen. (2015) Air Compressors for Fuel Cell Vehicles: An Systematic Review. *SAE International Journal of Alternative Powertrains*. 4. 10.4271/2015-01-1172.

[21] Demirel Y (2012) Energy: production, conversion, storage, conservation, and coupling. Springer Science & Business Media.

[22] Demirel Y (2018) 5.2 Energy Conservation in Dincer I *Comprehensive Energy Systems* (p.p. 45-90). Elsevier. https://doi.org/10.1016/B978-0-12-809597-3.00505-8.

[23] Park C-Y, Hong S-H, Lim S-C, Song B-S, Park S-W, Huh J-H, Kim J-C (2020) Inverter Efficiency Analysis Model Based on Solar Power Estimation Using Solar Radiation. *Processes*. 8(10) https://doi.org/10.3390/pr8101225

[24] https://www.doitpoms.ac.uk/tlplib/batteries/batteries_lithium.php#:~:text=Li%2Dion%20battery&text=Thus%20the%20maximum%20theoretical%20specific,components%20are%20taken%20into%20account.

[25] https://www.engineeringtoolbox.com/standard-atmosphere-d_604.html

[26] https://www.mide.com/air-pressure-at-altitude-calculator